

## **2D-Euler Deconvolution technique and Electrical Self-Potential analysis for subsurface structures delineation in Matuu, Machakos County, Kenya**

Odero E.O.<sup>1\*</sup>, K'Orowe M. O.<sup>1</sup>, Githiri J. G.<sup>1</sup>

<sup>1</sup>(Department of Physics, Jomo Kenyatta University of Agriculture and Technology, Nairobi)

---

**Abstract:** *In order to evaluate groundwater potential of Matuu-Kilango area faults and fractures which are groundwater conduits had to be delineated. Earlier use of geological reconnaissance report only in siting boreholes has led to recorded cases of borehole failure in Matuu. Integrated geophysical survey involving magnetics and electrical self-potential techniques was applied over a 25 square kilometre area. Qualitative interpretation involving generation of contour maps for magnetic anomaly as well as self-potentials was attempted. Euler Deconvolution solutions were obtained using a structural index of 0.5 that gave well clustered solutions and discontinuities over the anomalous zone. Fractured/faulted zone was identified to the west of Matuu-Kilango area with faults and fractures existing at 100m depth having general orientation of South-East to North-West. Along the faulted zone was prevalent negative self-potential values ranging from -10mV to about -100mV, an indication of availability of groundwater resource.*

**Keywords:** *Euler-Deconvolution, faults, Magnetic, Matuu area and self-potential.*

---

### **I. Introduction**

The Matuu-Kilango area is located in Yatta District, Machakos County approximately 110 km from Nairobi, 61.69 km from Thika town. The study area is bounded by latitudes 1° 05'S (9879000) and 1°08'S (9874000) and Longitudes 37° 31'E (335000) and 37° 33'E (340000) zone 37M as illustrated in Fig. 1. The area lies along the Eastern Mozambique Belt segment (EMBS) which stretches in our country (Kenya), about 800 km length and 200 km width at 3°N and 4°S latitudes and between 37°E and 39°E longitudes, [1]. In the study area, the surface rocks comprise of Metamorphic rocks which are overlain by the Yatta Plateau to the south. Matuu area is entirely underlain by Precambrian rocks of the basement system. The area of interest is located in Eastern side of Gregory Rift Valley. The area is largely semi-arid characterized by unreliable rainfall; moreover, given that the area is majorly made up of igneous rock formations its porosity is mainly secondary. This study was carried out with a view of delineating subsurface structures such as faults and fractures responsible for secondary porosity, a key factor in evaluation of groundwater potential and a control measure to losses from borehole failure due lack of understanding of the subsurface structures.

The study area has an underlying Precambrian basement crystalline rock system of Mozambique belt segment that have undergone through cycle of metamorphism, exposure and erosion. The surface rocks comprises of metamorphic rocks overlain by a Plateau (Yatta) to the south, the formation of Yatta plateau begun at the start of Miocene period by eruption of Phonolites. This resulted into large part sub-Miocene surface being covered by lava. This geological system only hold water in a network of fractures and faults since the metamorphic rocks are non-porous and impervious. The rock type is described by meta-intrusive mafic and ultramafic rocks that include Diorites, Gabbros, Anorthosites, Peridotites and Picrites. The mafic and ultra-mafic rocks occur in the general Machakos area and its environs, [2]. Inferred brittle/ductile fractures oriented in the North-West and South-East directions are found within the study area, the trends have been postulated to be due to escape of strain in the Mozambique belt rocks as a result of westward rigid craton collision, [3].

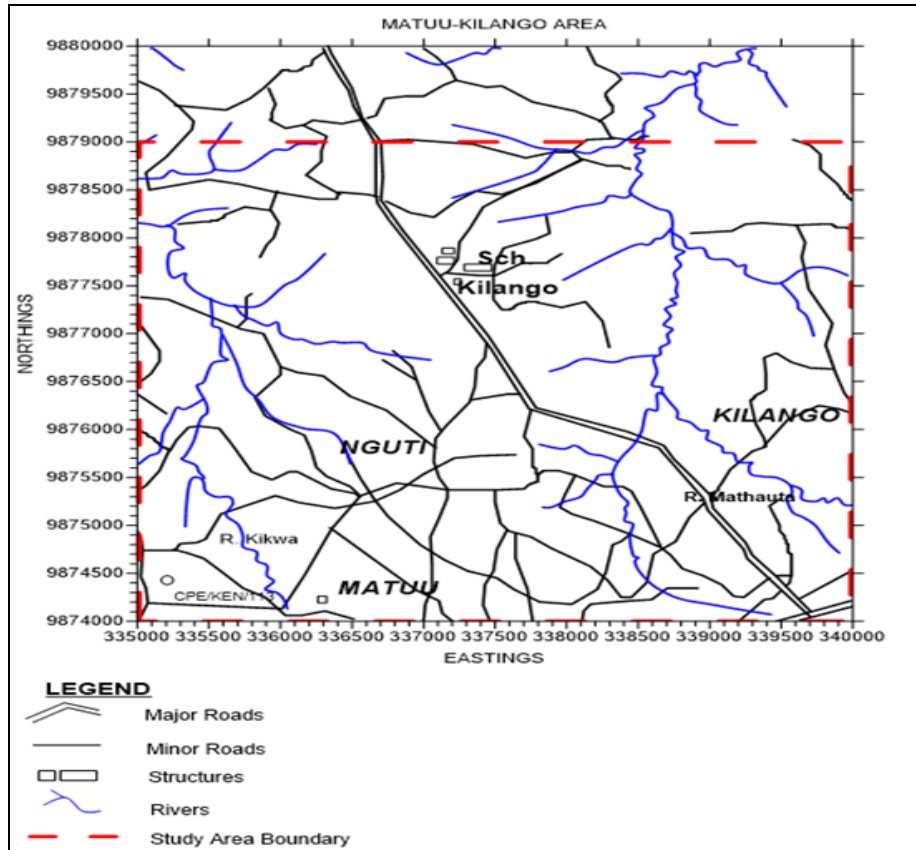


Figure 1: Location map of study area.

## II. 2d-Euler Deconvolution Technique

### 2.1 Theory

Other than Peter's Half-Slope method of subsurface depth estimations Euler deconvolution method is a more precise alternative since it operates on data directly and provide mathematical solutions without recourse to any geological constrains thus best for structural interpretations, [4]. By use of structural indices related to different magnetic sources and gradient of total magnetic field, Euler's equation (1) can be applied accurately to determine depth estimates of the sources where  $x_0$ ,  $y_0$ ,  $z_0$  are the coordinates of magnetic source whose total field intensity  $T$  and regional value  $B$  are measured at position defined by  $x$ ,  $y$ ,  $z$  with  $N$  as degree of homogeneity (structural index), [5].

$$(x - x_0) \frac{\partial T}{\partial x} + (y - y_0) \frac{\partial T}{\partial y} + (z - z_0) \frac{\partial T}{\partial z} = N(B - T) \quad (1)$$

In two dimensional cases, as for magnetic anomaly, the equation has only two unknowns  $x_0$  and  $y_0$  to be evaluated since  $N$  is theoretically known.  $N$  value between 0 and 1 is best for fault by magnetic method, [6]. Regions of clustered Euler solutions with discontinuities are normally of interest when delineating faults, [7].

### 2.2 Methodology

Geometrics 856 Proton Precession Magnetometer was used to measure total magnetic field to a resolution of 0.1nT. Ground magnetic data was collected in the S-N Direction along six straight profiles as shown in Fig. 2. The profiles were 5 km long each, with a distance separation of about 1 Km from each other.

Magnetic measurements were taken at every 200m meters station along each profile, with the base station readings taken after very two hours at a base station centrally located within the study area for diurnal corrections. A total of 189 measurement points were established and coordinates taken using a global positioning system (GPS), Data was subjected to diurnal and geomagnetic corrections and a total magnetic intensity contour map of contour interval of 50nT generated (Fig. 3), using Surfer 10 software.

From the contour plot of magnetic anomaly (Fig. 3), cross-sections AA', BB' and CC' were drawn. Anomaly data with linear variation defining the cross-sections were then uploaded into Euler 1.0 freeware.

Taking values of Geomagnetic Intensity, Inclination, Declination and sensor height for the study area to be 33,533.8nT,  $-23.0604^{\circ}$ ,  $0.4711^{\circ}$  and 4m respectively and the uploaded data was processed to obtain the plots labeled AA', BB' and CC'

The choice on what part of the map to cut cross-sections was controlled by the anomaly trends i.e. the western part of the area covered by the map indicates anomaly whose subsurface investigations are of interest.

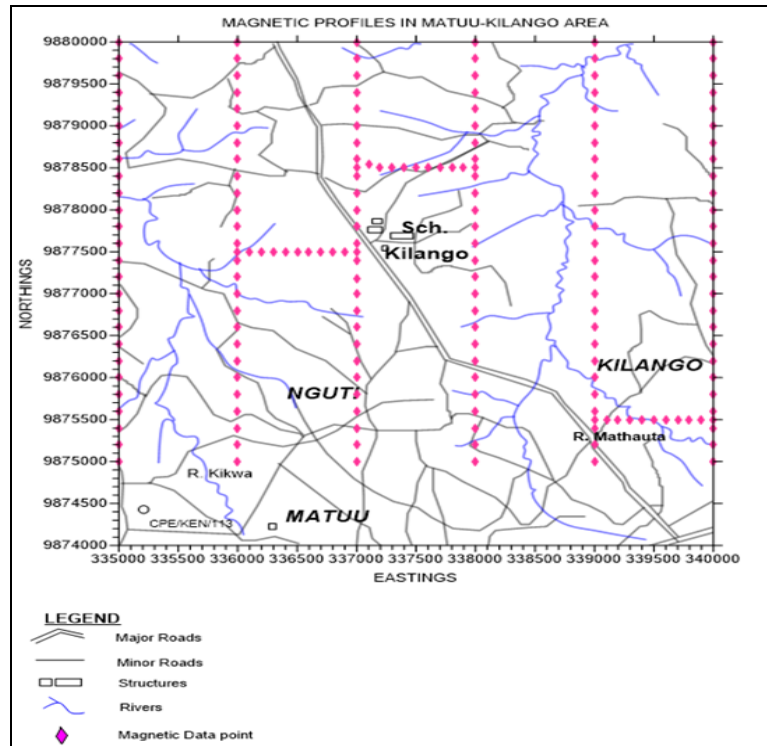


Figure 2: Magnetic measurement profiles over the study area: the shift to the North from northing 9874000 was an attempt of avoiding the magnetic noise effect from Matuu Town structures.

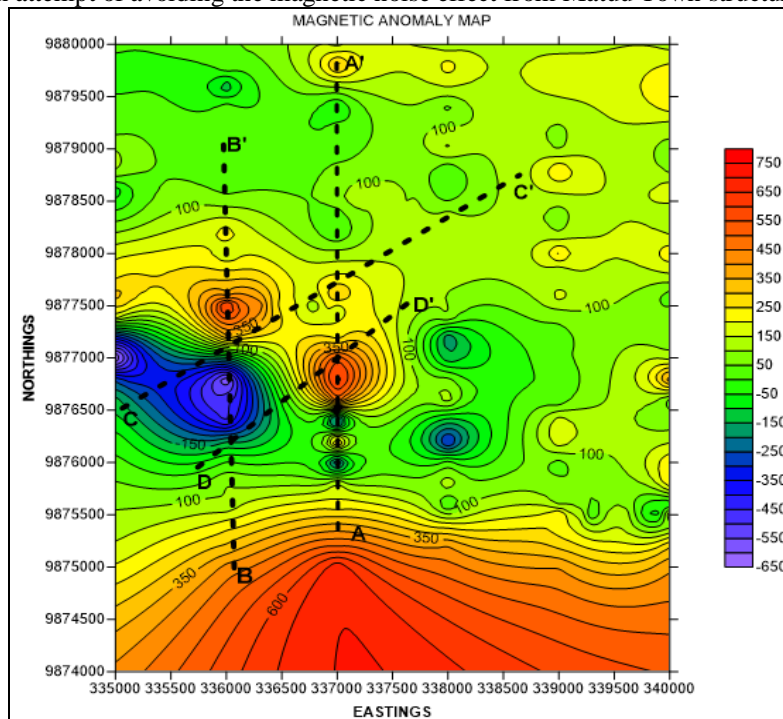


Figure 3: Total magnetic intensity contour map

### 2.3 Results and Discussion

Fig. 4 shows Euler solutions for magnetic profile AA' calculated using structural index of 0.5 which best represent faults. The horizontal and vertical gradients depict great fluctuations over 0.2km-1.5km profile distance representing lateral variations in magnetization over the same profile distance range. The depth to the source depicted by best clustered solutions is shallowest (about 100m) over the same distance range. A solution gap exist at the start of profile with no clear discontinuities shown for the rest of the profile an indication of possible fractures but no major fault.

From profile BB' shown in Fig. 5 is a result from Euler depth investigation using structural index of 0.5. For this section, the abrupt variation in horizontal and vertical gradients covers a wide range of profile distances, that is, from 1.2km to 2.75km along the profile. It is over this same region where shallowest (about 150m), best clustered Euler solutions and a disjointed formation at about 1.5km profile length was shown, an indication of the possible fault. The deepest solution to the basement is at about 400m from the surface.

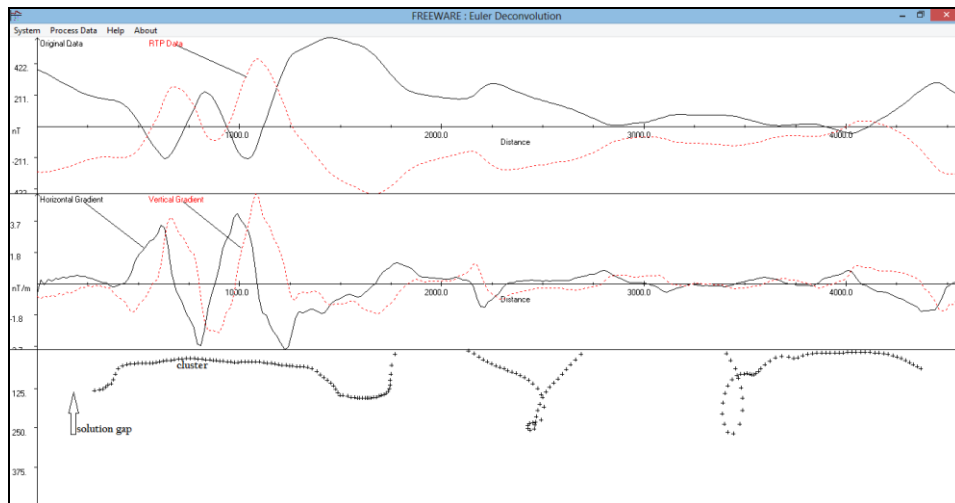


Figure 4: Profile AA' Euler depth solutions

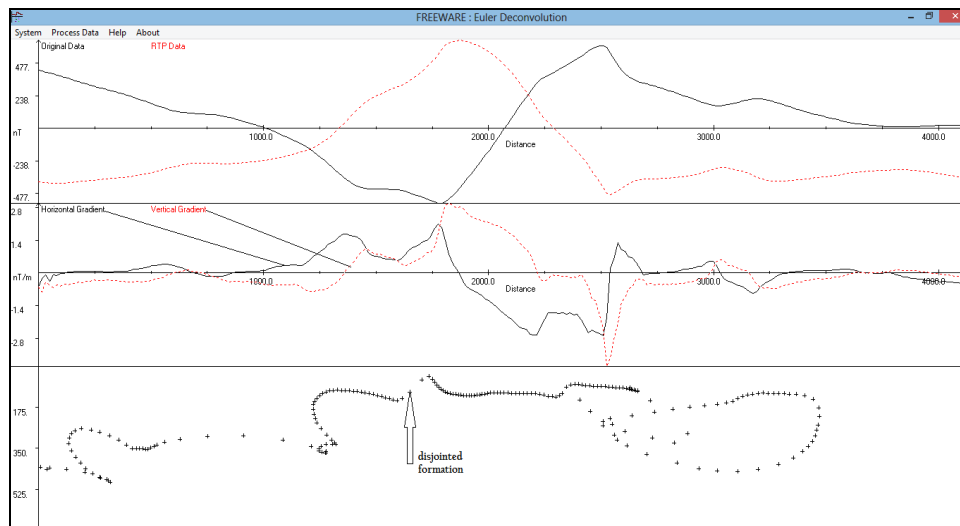
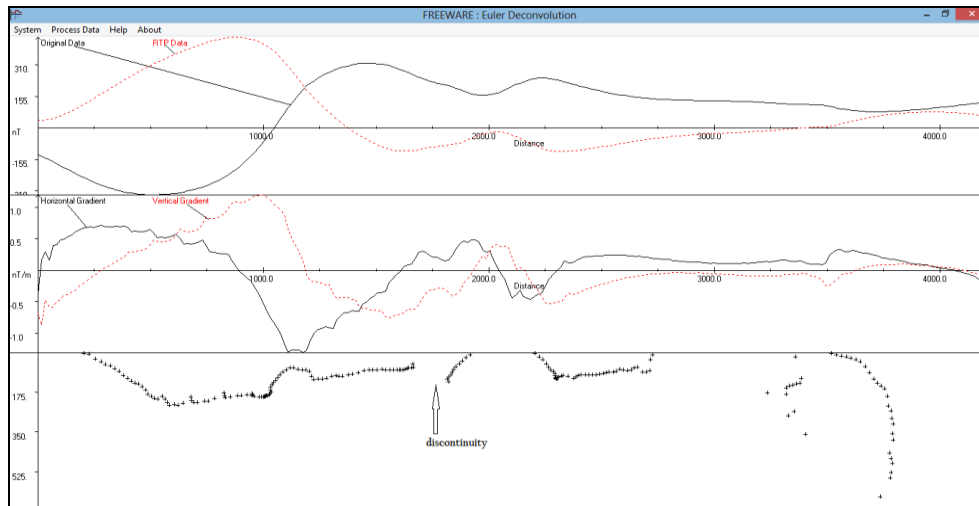


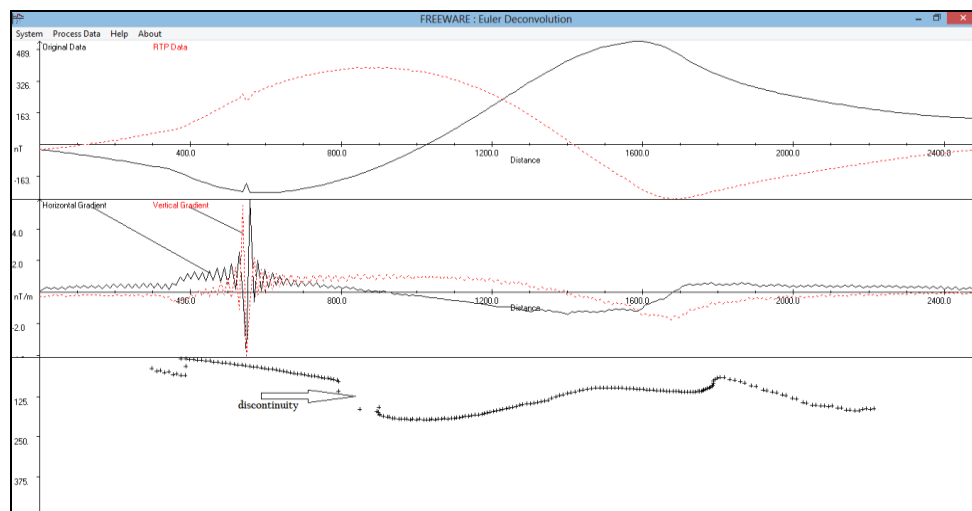
Figure 5: Profile BB' Euler depth solutions

Fig. 6 shows magnetic anomaly Euler solutions for profile CC'. A good image of subsurface structure depth was given by best cluster of solutions calculated using the most applicable structural index for fault (0.5) occurring averagely at 150m from the surface, at profile distances 0.2km to 2.75km with a clear discontinuity at about 1.8km distance along the profile showing an extension of the fault inferred in BB' Euler solution analysis. Horizontal and vertical gradients seemed to have begun varying abruptly a few meters from the start of the profile to a distance of 2.3km along the profile thus a wide variation in magnetisation.



**Figure 6:** Profile CC' Euler depth solutions

To verify the trends in Euler solution along the possible fault inferred from profiles BB' and CC' a profile DD' was drawn and Euler solutions determined (Fig. 7). It equally showed clustered solutions with a pronounced discontinuity at about 0.9km profile distance. The cluster extended up to 2.4km profile distance. The result helped in the inference of the fault orientation which appeared to be in SE-NW direction.



**Figure 7:** Profile DD' Euler depth solutions

### III. Electrical Self-Potential Method

#### 3.1 Theory

Self-potential (SP) or Spontaneous polarisation are potential differences resulting from natural subsurface processes e.g. groundwater movement, streaming fluids, and other subsurface geochemical reactions, [5]. The common factor among the various processes thought to be responsible for measured self-potentials is groundwater. The potentials are generated by flow of water, water acting as electrolyte and solvent of different minerals, moreover, negative self-potential values below -100mV is associated with groundwater, [4] and [8]. For a mineral body large negative anomalies can be observed, normally above -100mV. [5], describes the causative body to straddle water table below which electrolytes in the fluids undergo oxidation and release electrons which are conducted upwards through the ore body. At the top of the ore body the released electrons cause reduction of the electrolytes; a circuit thus exists with the top of the body acting as negative terminal thus negative SP anomalies observed.

The presence of streaming fluids or groundwater in a hard rock basement system can only be associated with secondary porosity originating from faults and fractures which act as groundwater conduits.

#### 3.2 Methodology

The measurements of SP only needed two electrodes and a voltmeter which is normally in built in most resistivity meters. Data points were identified randomly within the 25 square kilometre area (Fig. 1) coordinates

taken using GPS and self-potential readings taken using SARIS model resistivity meter. Electrode separation was kept constant at 50 meters. At least two readings were taken for each station and the averages recorded for analysis. The final data averages were uploaded to Surfer 10 software to develop a contour map with colour scale showing variation in self-potential values.

### 3.3 Results and Discussion

Fig. 8 shows variation of SP values over the study area. Qualitatively, the western area covered by the map depict a spread of negative SP values ranging from -10mV to about -100mV. The eastern side of the study area showed increasingly positive SP values. The trend of variation in negative SP values depicts an anomaly in the SE-NW direction an indication of weak geological structures in which groundwater accumulates. An anomalous body showing negative SP values above -100mV exist at the central zone and is associated with a conductive ore body in the subsurface.

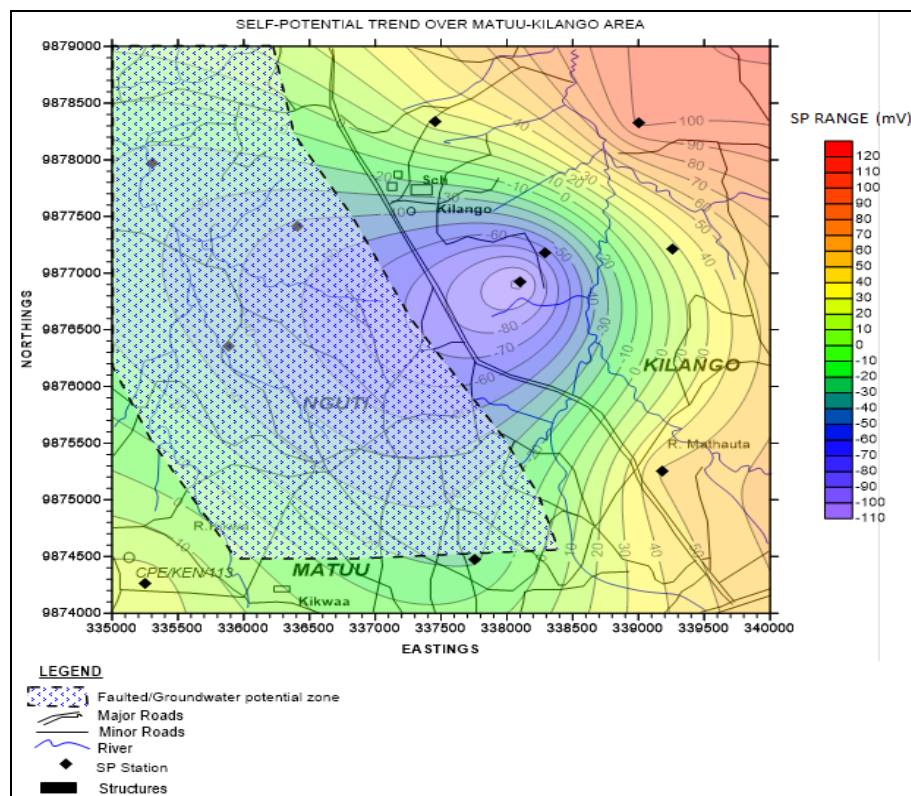


Figure 8: Self-Potential Contour map over the study area.

## IV. Conclusion And Recommendation

Recorded range of electrical self-potential values between -10mV to about -100mV in the western region of Matuu suggests presence of groundwater in the subsurface (Fig. 8). The area being underlain by crystalline hard rock system the presence of groundwater can only be as a result of secondary porosity by faulting and fracturing. These faults were delineated by Euler-deconvolution technique where with a structural index of 0.5 the depth of the fractured zone was found to be 100m from the surface. Considering the clustering of solutions and position of disjointed formation in profile BB', pronounced discontinuity along profile CC' and DD' it can be inferred that a fault exist in the western part of Matuu-Kilango area oriented in the SE-NW direction surrounded by numerous fractures responsible for percolation and accumulation of groundwater associated with negative self-potential values obtained in this study (Fig. 8). Towards the North-Western part of the study area, the depth to the structures slightly increases indicating an increasing thickness of faulted layer of the subsurface thus greater potential for groundwater accumulation. More survey work need to be done to the west of the study area to demarcate the extent of the fault over the area beyond the study area boundary.

### Acknowledgements

Special thanks to Society of Exploration Geophysicists Jomo Kenyatta University of Agriculture and Technology Chapter for field work assistance, Jomo Kenyatta University of Agriculture and Technology physics department for availing survey equipment as well as professional pieces of advice. This work was sponsored by Society of Exploration Geophysicist Foundation.

### References

- [1] E. Mathu, The Mutito faults in the Pan-African Mozambique Belt, Eastern Kenya, In Mason R. (Ed.), Basement Tectonics, (Netherlands, Kluwer Academics Publishers, 1992) 61-69.
- [2] C. Nyamai, E. Mathu, N. Opiyo-Akech and E. Wallbrecher, A reappraisal of the geology, geochemistry, structures and tectonics of the Mozambique Belt in Kenya: East of the Rift system. African Journal of Science and Technology, Science and Engineering series, 4(2), 2003, 51-71.
- [3] P. Mosley, Geological Evolution of the Late Proterozoic Mozambique Belt of Kenya, Tectonophys, 221, 1993, 223-250.
- [4] J. Reynolds, An Introduction to Applied and Environmental Geophysics (New York, John Wiley & Sons, 1998).
- [5] P. Keary, M. Brooks and I. Hill, An Introduction to Geophysical Exploration. (London, Blackwell Scientific Publications, 2002).
- [6] V. Grauch, R. Hudson, A. Minor and J. Caine, Sources of along-strike variation in magnetic anomalies related to intrasedimentary faults: A case study from the Rio Grande Rift, USA. Exploration Geophysics, 37, 2006, 372-378.
- [7] J. Githiri, J. Patel, J. Barongo and P. Karanja, Application of Euler Deconvolution Technique in determining depths to magnetic structures in Magadi Area, South Kenya Rift. Journal of Agriculture Science and Technology, 13(1), 2011, 142-156.
- [8] S. Jinadasa and R. Silva, Resistivity imaging and self-potential applications in groundwater investigations in hard crystalline rocks. Journal of the National Science Foundation of Sri Lanka, 37(1), 2009, 23-32.